

Efficient calculation of inelastic vibration signals in electron transport: Beyond the wide-band approximation

Jing-Tao Lü,^{1,2} Rasmus B. Christensen,² Giuseppe Foti,^{3,4}
Thomas Frederiksen,^{4,5} Tue Gunst,² and Mads Brandbyge²

¹*School of Physics, Huazhong University of Science and Technology, Wuhan, China*

²*Dept. of Micro- and Nanotechnology, Technical University of Denmark,
Ørsteds Plads, Bldg. 345E, DK-2800 Kongens Lyngby, Denmark*

³*Centro de Física de Materiales, Centro Mixto CSIC-UPV, Donostia-San Sebastián, Spain*

⁴*Donostia International Physics Center (DIPC) – UPV/EHU, Donostia-San Sebastián, Spain*

⁵*IKERBASQUE, Basque Foundation for Science, Bilbao, Spain*

(Dated: November 11, 2018)

We extend the simple and efficient lowest order expansion (LOE) for inelastic electron tunneling spectroscopy (IETS) to include variations in the electronic structure on the scale of the vibration energies. This enables first-principles calculations of IETS lineshapes for molecular junctions close to resonances and band edges. We demonstrate how this is relevant for the interpretation of experimental IETS using both a simple model and atomistic first-principles simulations.

PACS numbers: 73.63.-b, 68.37.Ef, 61.48.-c

The inelastic scattering of electronic current on atomic vibrations is a powerful tool for investigations of conductive atomic-scale junctions. Inelastic electron tunneling spectroscopy (IETS) has been used to probe molecules on surfaces with scanning tunneling microscopy (STM) [1], and for junctions more symmetrically bonded between the electrodes [2–7]. Typical IETS signals show up as dips or peaks in the second derivative of the current-voltage (I - V) curve [8]. In many cases the bonding geometry is unknown in the experiments. Therefore, first-principles transport calculations at the level of density functional theory (DFT) in combination with nonequilibrium Green’s functions (NEGF) [9–14] can provide valuable insights into the atomistic structure and IETS. For systems where the electron-vibration (e-vib) coupling is sufficiently weak and the density of states (DOS) varies slowly with energy (compared to typical vibration energies) one can greatly simplify calculations with the lowest order expansion (LOE) in terms of the e-vib coupling together with the wide-band approximation (LOE-WBA) [10, 15]. The LOE-WBA yields simple expressions for the inelastic signal in terms of quantities readily available in DFT-NEGF calculations. Importantly, the LOE-WBA can be applied to systems of considerable size.

However, the use of the WBA can not account for IETS signals close to electronic resonances or band edges, which often contains crucial information [16, 17]. For example, a change in IETS signal *from peak to peak-dip* shape was recently reported by Song *et al.* [6] for single-molecule benzene-dithiol (BDT) junctions, where an external gate enabled tuning of the transport from off-resonance to close-to-resonance. Also, high-frequency vibrations involving hydrogen appear problematic since the LOE-WBA is reported to underestimate the IETS intensity [18].

Here we show how the energy dependence can be in-

cluded in the LOE description without changing significantly the transparency of the formulas or the computational cost. We describe how the generalized LOE differs from the original LOE-WBA, and demonstrate that it captures the IETS lineshape close to a resonance. We apply it to DFT-NEGF calculations on the resonant BDT system and to off-resonant alkane-dithiol junctions, and show how the improved LOE is necessary to explain the experimental data.

Method. We adopt the usual two-probe setup with quantities defined in a local basis set in the central region (C) coupled to left/right electrodes ($\alpha = L, R$). We consider only interactions with vibrations (indexed by λ with energies $\hbar\omega_\lambda$ and e-vib coupling matrices \mathbf{M}_λ) inside C . To lowest order in the e-vib self-energies Σ_λ (2nd order in \mathbf{M}_λ) the current can be expressed as a sum of two terms, $I(V) = I_e + I_i$, using unperturbed Green’s functions $\mathbf{G}^a = \mathbf{G}^{r\dagger}$ defined in region C [10, 15],

$$I_e = \frac{G_0}{e} \int_{-\infty}^{\infty} d\varepsilon \{f_L(\varepsilon) - f_R(\varepsilon)\} \{\text{Tr}[\mathbf{G}^r \mathbf{\Gamma}_L \mathbf{G}^a \mathbf{\Gamma}_R](\varepsilon) + 2\text{Re} \text{Tr}[\mathbf{G}^r \Sigma_\lambda^r \mathbf{G}^r \mathbf{\Gamma}_L \mathbf{G}^a \mathbf{\Gamma}_R](\varepsilon)\}, \quad (1)$$

$$I_i = \frac{G_0}{e} \int_{-\infty}^{\infty} d\varepsilon \text{Tr}[\Sigma_\lambda^< \mathbf{G}^r \Sigma_L^> \mathbf{G}^a - \Sigma_\lambda^> \mathbf{G}^r \Sigma_L^< \mathbf{G}^a](\varepsilon), \quad (2)$$

where $G_0 = 2e^2/h$ is the conductance quantum and summation over the vibration index λ is assumed. The e-vib self-energies Σ_λ are expressed as

$$\Sigma_\lambda^{\gtrless}(\varepsilon) = \mathbf{M}_\lambda \left\{ (N_\lambda + 1) \mathbf{G}^{\gtrless}(\varepsilon_\mp) + N_\lambda \mathbf{G}^{\gtrless}(\varepsilon_\pm) \right\} \mathbf{M}_\lambda, \quad (3)$$

$$\Sigma_\lambda^{r,a}(\varepsilon) = \pm \frac{1}{2} \{ \Sigma_\lambda^>(\varepsilon) - \Sigma_\lambda^<(\varepsilon) \} - \frac{i}{2} \mathcal{H} [\Sigma_\lambda^> - \Sigma_\lambda^<](\varepsilon), \quad (4)$$

with $\varepsilon_\pm = \varepsilon \pm \hbar\omega_\lambda$, bosonic occupations N_λ , and \mathcal{H} denoting the Hilbert transform. Finally, the lesser/greater Green’s functions \mathbf{G}^{\gtrless} describing the oc-

cupied/unoccupied states,

$$\mathbf{G}^{\gtrless}(\varepsilon) = \mp i \{ f_L(\mp \varepsilon) \mathbf{A}_L(\varepsilon) + f_R(\mp \varepsilon) \mathbf{A}_R(\varepsilon) \}, \quad (5)$$

are given by the spectral density matrices $\mathbf{A}_\alpha = \mathbf{G}^r \mathbf{\Gamma}_\alpha \mathbf{G}^a$ for left/right moving states with fillings according to the reservoir Fermi-functions, $f_\alpha(\varepsilon) = n_F(\varepsilon - \mu_\alpha)$.

The above equations are numerically demanding because of the energy integration over *voltage-dependent* traces. In the following we describe how further simplifications are possible without resorting to the WBA. We are here interested in the “vibration-signal”, that is the change in the current close to the excitation threshold, $|eV| \approx \hbar\omega_\lambda$, with $eV = \mu_L - \mu_R$. As IETS signals are obtained at low temperatures, we assume that this is the smallest energy scale, $k_B T \ll \hbar\omega_\lambda, \Gamma$, where Γ is the typical electronic resonance broadening. The inelastic term I_i [Eq. (2)] then reduces to

$$I_i \approx \frac{G_0}{2e} \sum_{\sigma=\pm} \left(\coth \frac{\hbar\omega_\lambda}{2k_B T} - \coth \frac{\hbar\omega_\lambda + \sigma eV}{2k_B T} \right) \times \int_{-\infty}^{\infty} d\varepsilon \text{Tr} \left[\mathbf{M}_\lambda \tilde{\mathbf{A}}_L(\varepsilon) \mathbf{M}_\lambda \mathbf{A}_R(\varepsilon_\sigma) \right] \{ f_L(\varepsilon) - f_R(\varepsilon_\sigma) \}, \quad (6)$$

where $\tilde{\mathbf{A}}_\alpha = \mathbf{G}^a \mathbf{\Gamma}_\alpha \mathbf{G}^r$ is the time-reversed version of \mathbf{A}_α . In the 2nd derivative of I_i w.r.t. voltage V , the coth-parts give rise to a sharply peaked signal around $|eV| = \hbar\omega_\lambda$

with width of the order of $k_B T$. If the electronic structure (\mathbf{A}_α) varies slowly on the $k_B T$ scale, it can be replaced by a constant using $\varepsilon \approx \mu_L$ and $\varepsilon_\sigma \approx \mu_R = \mu_L + \sigma \hbar\omega_\lambda$. Thus, around the vibration threshold we get

$$\partial_V^2 I_i \approx \gamma_{i,\lambda} \partial_V^2 \mathcal{I}^{\text{sym}}, \quad (7)$$

$$\gamma_{i,\lambda} = \text{Tr} \left[\mathbf{M}_\lambda \tilde{\mathbf{A}}_L(\mu_L) \mathbf{M}_\lambda \mathbf{A}_R(\mu_R) \right], \quad (8)$$

where we, as in the LOE-WBA, define the “universal” function

$$\mathcal{I}^{\text{sym}} \equiv \frac{G_0}{2e} \sum_{\sigma=\pm} \sigma (\hbar\omega_\lambda + \sigma eV) \times \left(\coth \frac{\hbar\omega_\lambda}{2k_B T} - \coth \frac{\hbar\omega_\lambda + \sigma eV}{2k_B T} \right). \quad (9)$$

The elastic term I_e [Eq. (1)] can be divided in two parts, $I_e = I_e^n + I_e^h$, where the first(latter) represents all terms without(with) the Hilbert transformation originating in Eq. (4). The “non-Hilbert” part I_e^n yields a coth-factor and integral of similar in form to the one for I_i . Both I_i and I_e^n thus yield an inelastic signal with a lineshape given by the function $\partial_V^2 \mathcal{I}^{\text{sym}}$ and the sign/intensity governed by $\gamma_\lambda = \gamma_{i,\lambda} + \gamma_{e,\lambda}$, with $\gamma_{e,\lambda} \approx \text{Im}B_\lambda$, and

$$B_\lambda \equiv \text{Tr} [\mathbf{M}_\lambda \mathbf{A}_R(\mu_L) \mathbf{\Gamma}_L(\mu_L) \mathbf{G}^r(\mu_L) \mathbf{M}_\lambda \mathbf{A}_R(\mu_R) - \mathbf{M}_\lambda \mathbf{G}^a(\mu_R) \mathbf{\Gamma}_L(\mu_R) \mathbf{A}_R(\mu_R) \mathbf{M}_\lambda \mathbf{A}_L(\mu_L)]. \quad (10)$$

The “Hilbert” part I_e^h requires a bit more consideration. Besides terms which do not result in threshold signals [19], we have terms involving $\mathcal{H}[\mathbf{A}_\alpha f_\alpha]$. Again, if \mathbf{A}_α varies slowly around the step in f_α we may approximate

$$\mathcal{H}[\mathbf{A}_\alpha(\varepsilon') f_\alpha(\varepsilon')](\varepsilon) \approx \mathbf{A}_\alpha(\varepsilon) \mathcal{H}[f_\alpha(\varepsilon')](\varepsilon). \quad (11)$$

The Hilbert transformation of the Fermi function is strongly peaked at the chemical potential, and again

we evaluate the energy integral by evaluating all electronic structure functions ($\mathbf{A}_\alpha, \mathbf{G}^r, \mathbf{\Gamma}_\alpha$) at the peak values, keeping only the energy dependence of the functions related to f_α inside the integral. The result is

$$\partial_V^2 I_e^h \approx \kappa_\lambda \partial_V^2 \mathcal{I}^{\text{asym}}, \quad (12)$$

with $\kappa_\lambda = 2\text{Re}B_\lambda$ and, again as in the LOE-WBA, the “universal” function

$$\mathcal{I}^{\text{asym}} \equiv \frac{G_0}{2e} \int_{-\infty}^{+\infty} d\varepsilon \mathcal{H} \{ f(\varepsilon'_-) - f(\varepsilon'_+) \}(\varepsilon) (f(\varepsilon - eV) - f(\varepsilon)) \approx -\frac{G_0}{2e\pi} \sum_{\sigma=\pm} \sigma |eV + \sigma \hbar\omega_\lambda| \ln \left| \frac{eV + \sigma \hbar\omega_\lambda}{\hbar\omega_\lambda} \right|. \quad (13)$$

Here the latter is for $k_B T = 0$, while it can be expressed using the digamma function for finite $k_B T$ [20]. In total we have written the IETS as a sum of individual vibration

signals [10],

$$\partial_V^2 I(V) = \gamma_\lambda \partial_V^2 \mathcal{I}^{\text{sym}}(V, \hbar\omega_\lambda, T, N_\lambda) + \kappa_\lambda \partial_V^2 \mathcal{I}^{\text{asym}}(V, \hbar\omega_\lambda, T). \quad (14)$$

Equation (14) is our main formal result. As for the LOE-WBA we have expressed the vibration signals from the “universal” functions, and structure factors containing quantities readily obtained from DFT-NEGF. However, importantly, we have here generalized these to include the effect of *finite* $\hbar\omega_\lambda$, and thus the change in electronic structure over the excitation energy. Our LOE expressions for γ_λ and κ_λ above simply reduce to the LOE-WBA when $\mu_L = \mu_R = \mu_0$. We will now demonstrate some situations where the LOE expression Eq. (14) is crucial for detailed interpretation of experimental IETS lineshapes.

Simple model. First we use a single-level model to illustrate how the “asymmetric” term contains important information about the energy dependence of the electrode couplings. In the LOE-WBA one always has $\kappa_\lambda = 0$ for symmetric junctions. This is *not* the case for the LOE expression Eq. (10). We therefore consider a *symmetric junction* containing a single electronic level at ε_0 (with $\mu_0 = 0$), coupled to a local vibration (ω_0), and with energy-dependent electrode coupling rates. Assuming symmetrical potential drop, and using the notations $\Gamma_l = \Gamma_L(\mu_L) + \Gamma_R(\mu_L)$ and $\Gamma_r = \Gamma_L(\mu_R) + \Gamma_R(\mu_R)$ we can write the “symmetric”,

$$\gamma = -C \left\{ \Gamma_l^2 \Gamma_r^2 - (4\varepsilon_0^2 - \hbar^2 \omega_0^2)^2 \right\}, \quad (15)$$

and “asymmetric” coefficients,

$$\kappa = 4C (\delta\Gamma \varepsilon_0 + \bar{\Gamma} \hbar\omega_0) \left\{ \Gamma_l \Gamma_r - (4\varepsilon_0^2 - \hbar^2 \omega_0^2) \right\}, \quad (16)$$

where $\delta\Gamma = \Gamma_l - \Gamma_r$, $\bar{\Gamma} = (\Gamma_l + \Gamma_r)/2$, and C a constant common to γ and κ . In the typical case of transition metal electrodes the coupling can contain contributions both from a wide *s*-band as well as from a narrow *d*-band leading to a significant $\delta\Gamma$ and finite κ . To model the *s*-band we use a constant Γ_0 , and to mimic the coupling (hopping t') to a *d*-band we add the self-energy of a semi-infinite 1D chain, with bandwidth $2W$ centered at $\mu_0 = 0$. Figure 1 (a-c) compares the signals calculated from LOE-WBA and LOE for different ε_0 . For both treatments we observe that the peak in the off-resonance IETS evolves into a dip on-resonance. However, only in the LOE the two regimes are separated by a peak-dip structure close to resonance due to the “asymmetric” κ , which is enhanced at the onset of the coupling with *d* band in one electrode. The change in IETS signal with a gate-potential (ε_0) is shown in Fig. 1 (d). The features observed at $\varepsilon_0 = \pm\hbar\omega/2 - W$ is associated with the level being resonant with the left/right *d*-band onset, respectively.

IETS of benzene-dithiol. It has been possible to apply an external gate potential to junctions with small molecules between metallic electrodes [5, 6]. Under these conditions IETS have been recorded for gated octane-dithiol (ODT) and benzene-dithiol (BDT) molecules between gold electrodes [6]. For both ODT and BDT the

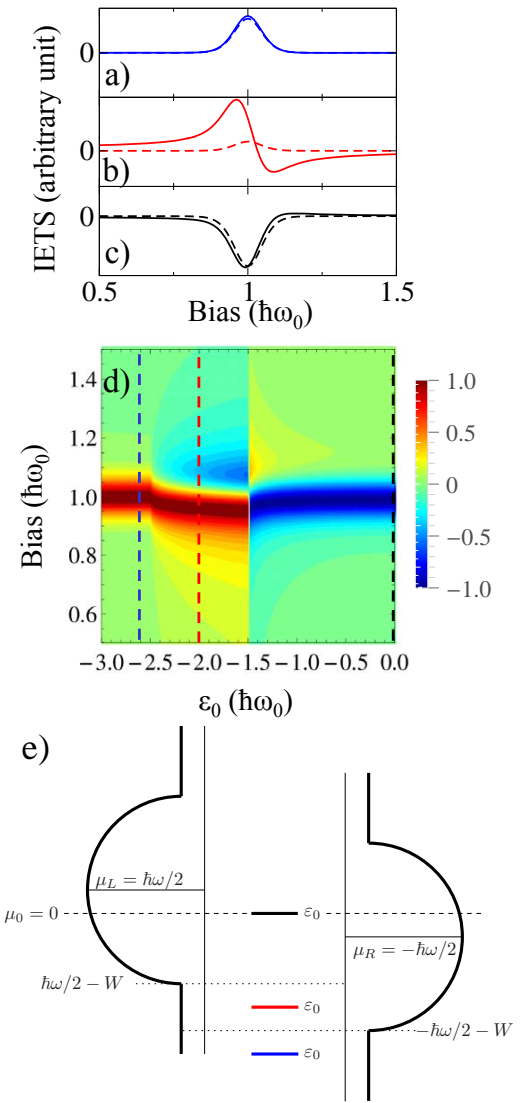


FIG. 1: (color online) (a-c) IETS spectrum from LOE (solid) and LOE-WBA (dashed) for three different position of an electronic level, coupling with a wide *s* band with constant density of states, and a narrow *d* band with bandwidth W centered at the equilibrium Fermi level $\mu_0 = 0$. (a) $\varepsilon_0 = -2.6$, (b) $\varepsilon_0 = -2$, (c) $\varepsilon_0 = 0$. The transmission coefficients at the Fermi level are $T = 0.006, 0.01, 1$, respectively. (d) Contour plot of the IETS spectrum for different level positions. The signal is normalized such that for each given ε_0 , the height of the largest peak or dip is 1. Parameters in unit of the vibration energy $\hbar\omega_0$: $t' = 2t = W = 2$, $\Gamma_0 = 0.1$, $k_B T = 0.02$. Here, t is the hopping matrix element of the *d* band, and t' is its coupling to the electronic level. (e) Schematics of the one-level model (shown for the three different level positions) biased at the emission threshold $V = \hbar\omega$.

quite symmetric *I*–*V* characteristics indicates a symmetric bonding to the electrodes. For the π -conjugated BDT it was shown how the transport can be tuned from far off-resonance ($G \sim 0.01G_0$) to close to the HOMO resonance increasing the conductance by more than an order

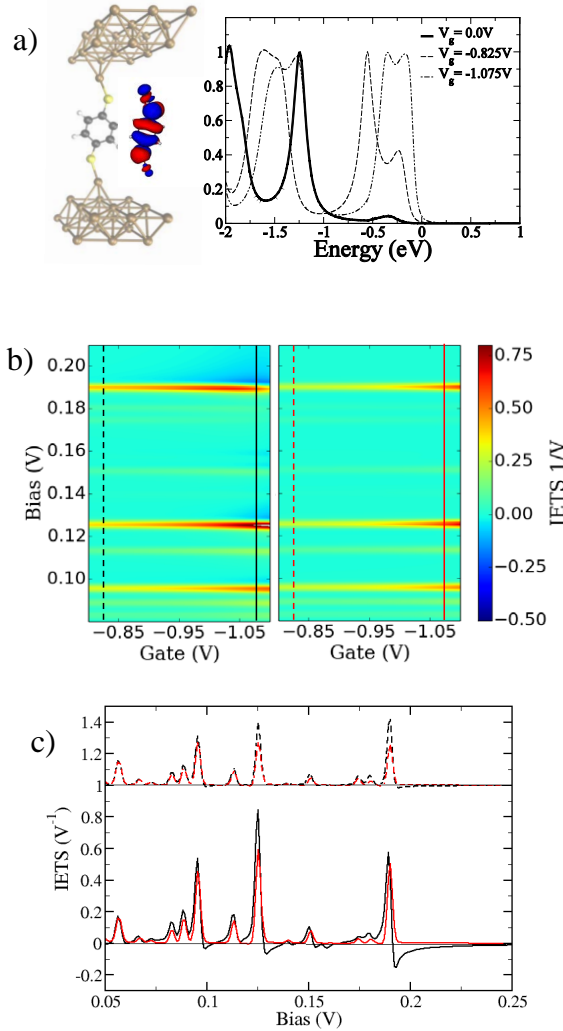


FIG. 2: (color online) (a) BDT between two adatoms on Au(111) together with transmission for off resonance (zero gate) and close to resonance. (b) IETS as a function of gate voltage from LOE (left) and LOE-WBA (right). (c) IETS for fixed gate voltage off-resonance (dashed lines, offset for clarity) and close-to-resonance (solid lines). Black: LOE, Red: LOE-WBA. The IETS signals are calculated for $T = 4.2$ K and processed to mimic the experimental broadening arising from the lock-in technique with a harmonic voltage modulation of $V_{\text{rms}} = 5$ mV [13].

of magnitude. As in the simple symmetric model above, this was reflected in the shape of the IETS signal for BDT going from a peak for off-resonance, to a peak-dip close to resonance, with the peaks appearing at the same voltages. However, the analysis by Song *et al.* [6] was based on a model assuming asymmetric electrode couplings at zero bias (STM regime) [16]. Our simple model [Fig. 1(b)] instead suggests that the observed peak-dip lineshape originates solely from the Γ_L, Γ_R asymmetry driven by the bias voltage near resonance rather than

from asymmetric electrode couplings (Γ_L, Γ_R).

Next, we turn to our DFT-NEGF calculations [27]. The importance of an efficient scheme is underlined by the fact that an IETS calculation is required for each gate value. In the break-junction experiments the atomic structure of the junction is unknown. We anticipate that the gap between the electrodes is quite open and involves sharp asperities with low-coordinated gold atoms in order to allow for the external gating to be effective. In order to emulate this, we consider BDT bonded between adatoms on Au(111) surfaces [Fig. 2(a)], and employ only the Γ -point in the transport calculations yielding sharper features in the electronic structure. We correct the HOMO-LUMO gap [21] and model the electrostatic gating simply by a rigid shift of the molecular orbital energies relative to the gold energies. In Fig. 2(b)-(c) we compare IETS calculated with LOE and LOE-WBA as a function of gating. As in the experiment, we observe three clear signals around $\hbar\omega = 95, 130, 200$ meV due to benzene vibrational modes. Off resonance, the LOE and LOE-WBA are in agreement as expected. But when the gate voltage is tuned to around $V_g \approx -1$ V the methods deviate because of the appearance of sharp resonances in the transmission around the Fermi energy [Fig. 2(a)]. These resonances involve the d -orbitals on the contacting gold atoms, as seen in the eigenchannel [22] plot in Fig. 2(a), and result in a peak-dip structure as seen in the experiment and anticipated by the simple model. Thus it is important to go beyond LOE-WBA in order to reproduce the peak to peak-dip transition taken as evidence for close-to-resonance transport.

IETS of alkane-dithiol. As another demonstration of the improvement of LOE over LOE-WBA, we consider molecular junctions formed by straight or tilted butane-dithiol (C4DT) molecules linked via low-coordinated Au adatoms to Au(111) electrodes, see inset to Fig. 3. Based on DFT-NEGF [27] we calculate elastic transmission and IETS for the periodic structure averaged over electron momentum k_{\parallel} [23]. As shown in Fig. 3(a)-(b), transport around the Fermi level is off-resonance but dominated by the tail of a sulfur-derived peak centered at approximately 0.25 eV below the Fermi level. This feature introduces a relatively strong energy-dependence into the electronic structure which makes the WBA questionable. Indeed, as shown in Fig. 3(c), LOE-WBA gives a smaller IETS intensity compared to the LOE for the energetic CH_2 stretch modes ($\hbar\omega \sim 375$ meV). The WBA may thus be the reason why LOE-WBA calculations were reported to underestimate the IETS intensity for these energetic modes in comparison with experiments [18]. We note that the intensity enhancement is found to be more pronounced for the straight configuration, which may be rationalized from Eq. (15) (the condition $\varepsilon_0 = \pm\hbar\omega_0/2$ better describes the vertical than the tilted case). The intensity change reported in Fig. 3 thus suggests the relevance of going beyond LOE-WBA for simulations involv-

ing high-energy vibrational modes.

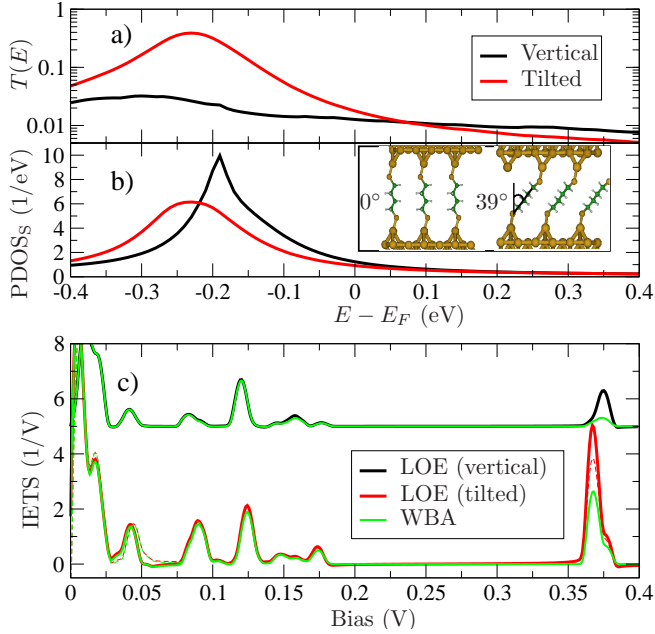


FIG. 3: (color online) (a) Transmission and (b) projected density of states over S for vertical and tilted C4DT in a 2×2 supercell of Au(111). (c) IETS within LOE and LOE-WBA (averaged over $k_{||}$) using $T = 4.2$ K and $V_{\text{rms}} = 5$ mV [13]. Thin dashed lines represent the reverse bias polarity.

Conclusions. A generalized LOE scheme for IETS simulations with the DFT-NEGF method has been described. Without introducing the WBA, our formulation retains both the transparency and computational efficiency of the LOE-WBA. This improvement is important to capture correctly the IETS lineshape in situations where the electronic structure varies appreciably on the scale of the vibration energies, such as near sharp resonances or band edges. Together with DFT-NEGF calculations we have discovered that the intricate experimental lineshape of a gated BDT can be explained without the need to assume asymmetric bonding of the molecule to the electrodes. Also, simulations for C4DT junctions suggest that going beyond WBA is important to capture the IETS intensity related to energetic CH_2 stretch modes.

We acknowledge computer resources from the DCSC. JTL acknowledges support from the National Natural Science Foundation of China (Grant No. 11304107, 61371015), and the Fundamental Research Funds for the Central Universities (HUST:2013TS032). GF and TF acknowledge support from the Basque Departamento de Educación and the UPV/EHU (Grant No. IT-756-13), the Spanish Ministerio de Economía y Competitividad (Grant No. FIS2010-19609-C02-00), and the European Union Integrated Project PAMS.

- [1] B. C. Stipe, M. A. Rezaei, and W. Ho, *Science* **280**, 1732 (1998).
- [2] N. Agrait, C. Untiedt, G. Rubio-Bollinger, and S. Vieira, *Phys. Rev. Lett.* **88**, 216803 (2002).
- [3] R. H. M. Smit, Y. Noat, C. Untiedt, N. D. Lang, M. C. van Hemert, and J. M. van Ruitenbeek, *Nature (London)* **419**, 906 (2002).
- [4] J. G. Kushmerick, J. Lazarcik, C. H. Patterson, R. Shashidhar, D. S. Seferos, and G. C. Bazan, *Nano Lett.* **4**, 639 (2004).
- [5] L. H. Yu, Z. K. Keane, J. W. Ciszek, L. Cheng, M. P. Stewart, J. M. Tour, and D. Natelson, *Phys. Rev. Lett.* **93**, 266802 (2004).
- [6] H. Song, Y. Kim, Y. H. Jang, H. Jeong, M. A. Reed, and T. Lee, *Nature* **462**, 1039 (2009).
- [7] N. Okabayashi, M. Paulsson, and T. Komeda, *Prog. Surf. Sci.* **88**, 1 (2013).
- [8] M. Galperin, M. A. Ratner, and A. Nitzan, *J. Phys.: Condens. Matter* **19**, 103201 (2007).
- [9] N. Sergueev, D. Roubtsov, and H. Guo, *Phys. Rev. Lett.* **95**, 146803 (2005).
- [10] M. Paulsson, T. Frederiksen, and M. Brandbyge, *Phys. Rev. B* **72**, 201101 (2005).
- [11] J. Jiang, M. Kula, W. Lu, and Y. Luo, *Nano Lett.* **5**, 1551 (2005).
- [12] G. C. Solomon, A. Gagliardi, A. Pecchia, T. Frauenheim, A. Di Carlo, J. R. Reimers, and H. S. Hush, *J. Chem. Phys.* **124**, 094704 (2006).
- [13] T. Frederiksen, M. Paulsson, M. Brandbyge, and A.-P. Jauho, *Phys. Rev. B* **75**, 205413 (2007).
- [14] E. T. R. Rossen, C. F. J. Flipse, and J. I. Cerdá, *Phys. Rev. B* **87**, 235412 (2013).
- [15] J. K. Viljas, J. C. Cuevas, F. Pauly, and M. Hafner, *Phys. Rev. B* **72**, 245415 (2005).
- [16] B. N. J. Persson and A. Baratoff, *Phys. Rev. Lett.* **59**, 339 (1987).
- [17] R. Egger and A. O. Gogolin, *Phys. Rev. B* **77**, 113405 (2008).
- [18] N. Okabayashi, M. Paulsson, H. Ueba, Y. Konda, and T. Komeda, *Nano Lett.* **10**, 2950 (2010).
- [19] F. Haupt, T. Novotny, and W. Belzig, *Phys. Rev. B* **82**, 165441 (2010).
- [20] G. Bevilacqua (2013), arXiv:1303.6206 [math-ph].
- [21] V. M. García-Suárez and C. J. Lambert, *New Journal of Physics* **13**, 053026 (2011).
- [22] M. Paulsson and M. Brandbyge, *Phys. Rev. B* **76**, 115117 (2007).
- [23] G. Foti, D. Sanchez-Portal, A. Arnau, and T. Frederiksen, (in preparation).
- [24] J. M. Soler, E. Artacho, J. D. Gale, A. Garcia, J. Junquera, P. Ordejón, and D. Sanchez-Portal, *J. Phys.: Condens. Matter* **14**, 2745 (2002).
- [25] M. Brandbyge, J. L. Mozo, P. Ordejón, J. Taylor, and K. Stokbro, *Phys. Rev. B* **65**, 165401 (2002).
- [26] J. P. Perdew, K. Burke, and M. Ernzerhof, *Phys. Rev. Lett.* **77**, 3865 (1996).
- [27] We employ the SIESTA [24]/TranSIESTA [25] method with the GGA-PBE [26] exchange-correlation functional. Electron-vibration couplings and IETS are calculated with Inelastica [13].